

# Basics of NMR

Dr. Albert A. Smith-Penzel

28 April, 2020

## 1 Early History of Magnetic Resonance

Magnetism was known to the ancient world, where lodestones would attract iron. In the modern world, macroscopic magnets serve a variety of practical purposes, from navigation, electric motors, electricity generation, magnetic levitation, or simply holding things up on the refrigerator. Each of these applications uses the collective effects of many "spins" (electron spins) acting together to create a large, macroscopic force. In this course, we will see how "spin" (nuclear spin, rather than electron spin) may be used to investigate structure and dynamics of biomolecules. We start with a brief history of spin.

### 1.1 Spin

The Stern-Gerlach experiment (1922) first showed that single particles have a quantized angular momentum [1].

- Particles (silver atoms) are sent through a magnetic field gradient, and deflect depending on the direction of the magnetic moment of the particle.
- To understand this experiment, consider what would happen if, instead of the single particle, one had a bar magnet. As the magnet travels through the field gradient, if the external magnetic field and the bar magnet are aligned (thus repelling each other), the bar magnet will be deflected towards the weaker field (where the bar magnet is less repelled by the field). If the magnetic field and bar magnet point in opposite directions, the bar magnet will deflect towards the stronger field (where the bar magnet is more attracted to the field). In-between orientations are also possible, resulting in a lesser degree of deflection, so that the amount of deflection may fall anywhere between the maximum and minimum (Figure 1A).
- This is not what is observed for a single particle, however. Instead, only the maximum and minimum deflection is observed, showing that the angular momentum is quantized, that is, there are only possible states of the electron are 1) parallel with the field or 2) anti-parallel with the field having (Figure 1B).
- The quantized angular momentum demonstrated by the Stern-Gerlach experiment turns out to be the fourth quantum number postulated by Wolfgang Pauli (1925), in his exclusion principle (one electron per quantum state, where the fourth quantum number has two possible values [2]). Goudsmit and Uhlenbeck's idea of electron spin eventually turned out to be this fourth quantum number, and is given values of  $m_s = \pm \frac{1}{2}$  [3].
- These two states of the electron, that is, spin up ( $m_s = \frac{1}{2}$ ) and spin down ( $m_s = -\frac{1}{2}$ ) have different energy levels when placed in a magnetic field, where

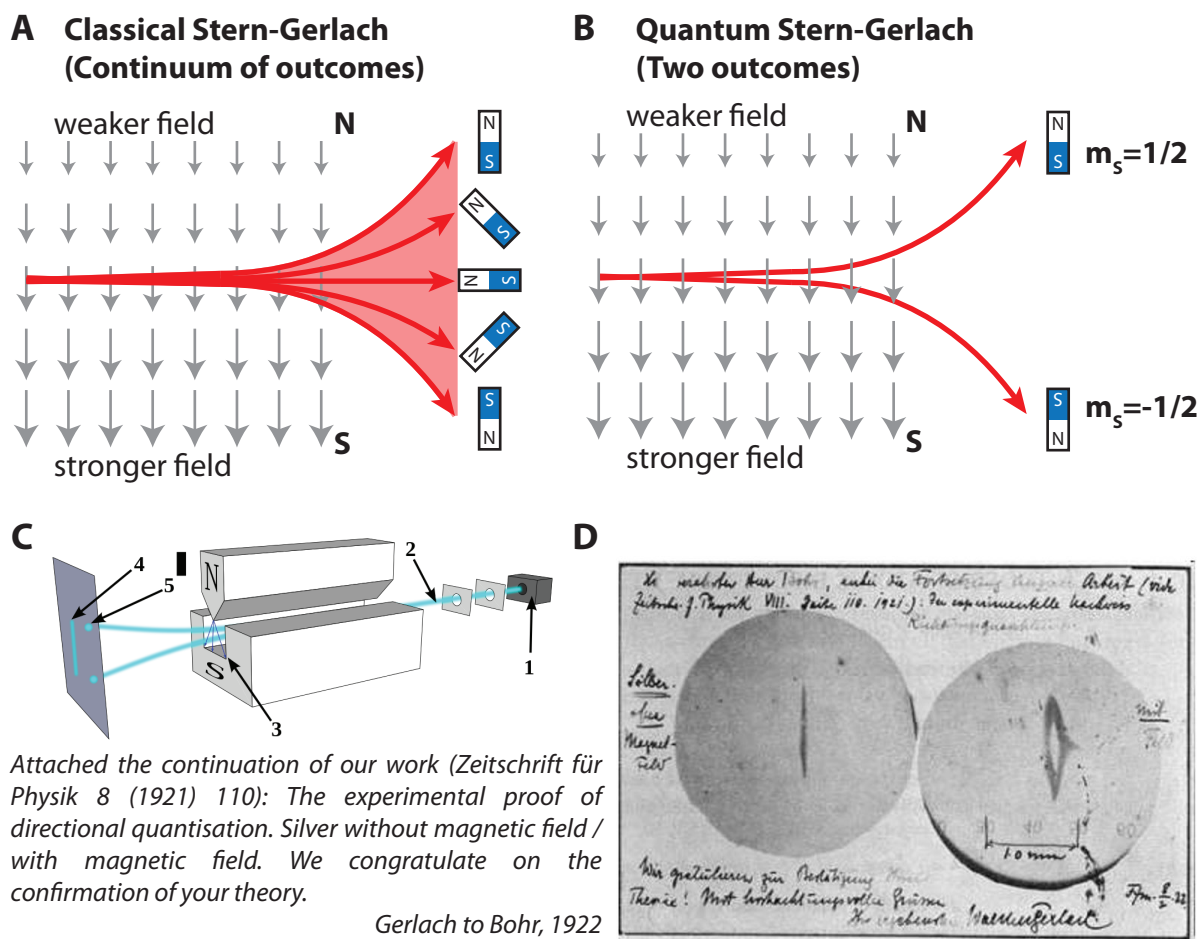


Figure 1: Stern-Gerlach Experiment. **A** shows the trajectory of several bar magnets of different orientations through a magnetic field gradient (larger arrows indicate a stronger field). **B** shows the trajectory of single particles with quantized states ( $S = \pm \frac{1}{2}$ ), where only two outcomes are possible. **C** shows a schematic of the Stern-Gerlach apparatus. Particles travel from the source (1) and through an aperture (2), through the magnet which yields a field gradient at (3) to a detector (4), where only two positions are observed (5). **D** shows the results on a postcard from Gerlach to Niels Bohr (translation to left), where a single line of particles is detected without magnetic field, but that line is split into two when a magnetic field gradient is applied (text of postcard translated to the left).

the difference in energy is proportional to the size of the magnetic field. This is known as the Zeeman effect.

- Like the electron, protons and neutrons also have two spin states ( $m_s = \pm \frac{1}{2}$ ). Nuclei, which contain one or more protons and neutrons, may also have  $I > 1/2$ , since multiple  $I = 1/2$  particles act as a single spin ( $I$  is not simply the sum of the individual spin-1/2 particles, however).
- The spin ( $I$ ) of several nuclei important to NMR are given in Table 1. Possible spin states for each value of  $m_I$  are  $-I, -I + 1, \dots, I$  (for  $I = 0, m_I = 0; I = 1/2, m_I = -1/2, 1/2; I = 1, m_I = -1, 0, 1$ ; and so on). That is, for a particle with spin  $I$ , there are  $2I + 1$  possible states. In this course, we will focus on spectroscopy using  $^1\text{H}$ ,  $^{13}\text{C}$ , and  $^{15}\text{N}$  nuclei, and so will always have  $I = 1/2$ , and therefore two possible states  $m_I = \pm 1/2$ .

Table 1: Important isotopes for NMR spectroscopy

Isotope	Spin ( $I$ )	Natural abundance [%]	NMR Frequency at $B_0=2.3488$ T	Gyromagnetic ratio, $\gamma$ $10^7 \text{ rad} \cdot T^{-1} \cdot s^{-1}$
$^1\text{H}$	1/2	99.98	100.000	26.7519
$^2\text{H}$	1	0.016	15.351	4.1066
$^3\text{H}$	1/2	–	106.663	28.535
$^{10}\text{B}$	3	19.58	10.746	2.8746
$^{11}\text{B}$	3/2	80.42	32.084	8.5843
$^{12}\text{C}$	0	98.9	–	–
$^{13}\text{C}$	1/2	1.108	25.144	6.7283
$^{14}\text{N}$	1	99.63	7.224	1.9338
$^{15}\text{N}$	1/2	0.37	10.133	-2.712
$^{16}\text{O}$	0	99.96	–	–
$^{17}\text{O}$	5/2	0.037	13.557	-3.6279
$^{19}\text{F}$	1/2	100	94.077	25.181
$^{29}\text{Si}$	1/2	4.70	19.865	-5.3188
$^{31}\text{P}$	1/2	100	40.481	10.841

## 1.2 Resonance

So where does that leave us? We have the property of spin, present both for electrons and nuclei. That spin is quantized, so that for a nucleus with spin  $I$ , only the spin states  $m_I = -I, -I + 1, \dots, I$  are allowed. If a spin is in a magnetic field, furthermore, the difference in energy of these spin states is (approximately)

$$\Delta E = \hbar \gamma B_0, \quad (1)$$

where  $\gamma$  depends on what type of nucleus is placed in the field (Table 1, 5th column), and  $B_0$  is the strength of the magnetic field itself.

- In 1938, Isidor Rabi showed that by irradiating at the frequency corresponding to the difference in energy of the two spin states, he could cause the spin state to change ( $m_S = -1/2 \rightarrow 1/2$  or  $m_S = 1/2 \rightarrow -1/2$ ) [4].
- Rabi prepared an apparatus where an  $S = 1/2$  particle (LiCl) is sent through a field gradient, causing the particle to deflect depending on the spin state ( $m_S = \pm 1/2$ ), as in the Stern-Gerlach experiment. However, the gradient is then reversed later along the path of the particle, deflecting in the opposite direction allowing the particle to refocus and arrive at a detector. This is illustrated in Figure 2.
- When an oscillating field, with frequency  $\omega = \gamma B_0$  ( $\hbar \omega = \Delta E$ ) is applied along the trajectory of the particle, the number of particles at the detector is reduced. This happens because the applied field causes the spin state to change, so the deflection of the particle continues in the same direction and the particle is no longer detected. This spin-state change was the first demonstration of magnetic resonance (resonance, because one matches the frequency of the oscillating field to the natural oscillation frequency of the electron).
- A modern magnetic resonance experiment does not require a particle to travel through a field gradient. Instead, a single coil is used both to apply oscillating magnetic fields to a nuclear spins that are in the sample (in a uniform magnetic field), and to measure oscillating fields resulting from the nuclear spins in the sample itself.

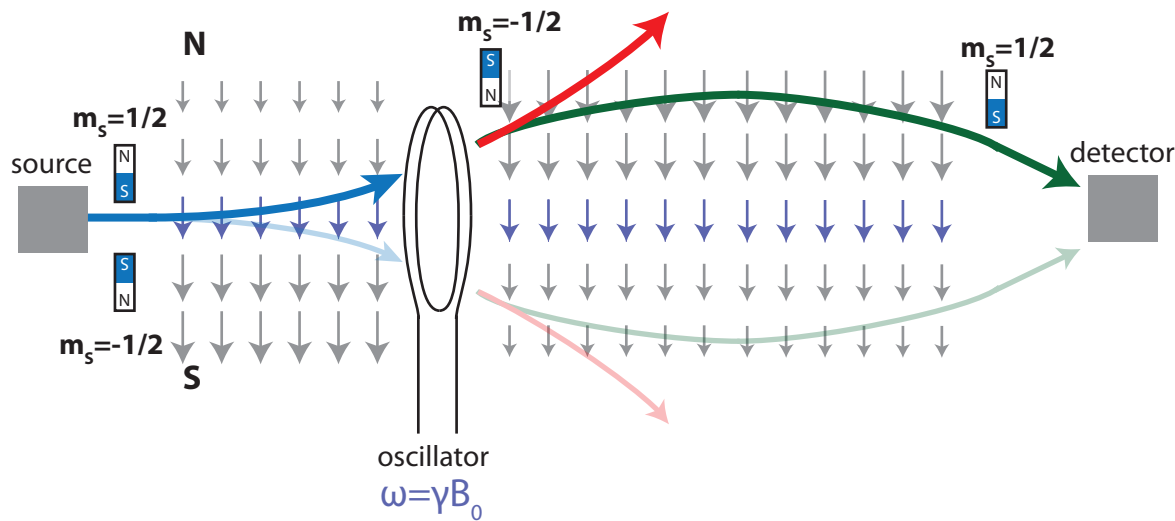


Figure 2: Rabi magnetic resonance experiment. A particle ( $S = 1/2$ ) is sent through a field gradient. It initially deflects up or down, depending on  $m_s$  (blue path). A second, inverted gradient, deflects the particle in the opposite direction so that it arrives at the detector (green path). However, if an oscillating magnetic field is applied at the oscillator with angular frequency  $\omega = \gamma B_0$ , then the spin state is switched ( $m_s = -1/2 \rightarrow 1/2$  or  $m_s = 1/2 \rightarrow -1/2$ ), and the particle continues to deflect in the same direction, failing to arrive at the detector (red path).

## 2 Spins in a Magnetic Field

This brings us to the behavior of spins in a magnetic field, where a static field ( $B_0$ , Figure 3A) is produced by a large superconducting magnet ( 5-24 Tesla) and oscillating fields are produced with a coil ( $B_1$  Figure 3B). We will consider how magnetization evolves in time, and how one may manipulate the magnetization in a sample. The simplest approach to grasping the behavior of magnetization in NMR is the Bloch equations [5].

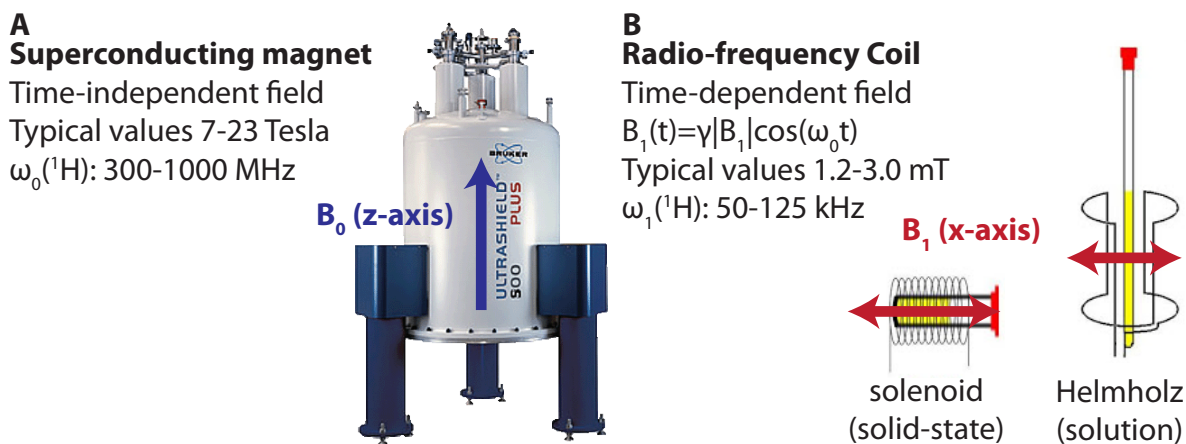


Figure 3: Source of  $B_0$  and  $B_1$  fields. **A** Superconducting magnets are used to produce large, homogeneous static  $B_0$  fields. Typically, we define the z-axis to be in the same direction as the  $B_0$  field. **B** A wire coil is used to produce an oscillating magnetic field, and also to measure the magnetic field produced by the ensemble of spins (nuclei) in the sample. The oscillating field is 3-4 orders of magnitude smaller than the  $B_0$  field. The coil is connected first to a tuned radio-frequency circuit, which attaches to an NMR console, which both produces oscillating pulses and can detect oscillations produced in the coil by the sample.

## 2.1 The Bloch Equations

In NMR, we do not observe single spins, but rather "ensembles" of equivalent spins. Then, it makes sense to describe the average magnetization of these ensembles (where the ensemble corresponds to a particular atom in a molecule, where many copies of that molecule are in solution and so one observes the spin of that atom many times). The Bloch equations describe the evolution of this average magnetization for a time-dependent magnetic field.

$$\begin{aligned}
 \frac{dM_x(t)}{dt} &= \gamma(M_y(t) * B_z(t) - M_z(t) * B_y(t)) - \frac{M_x(t)}{T_2} \\
 \frac{dM_y(t)}{dt} &= \gamma(M_z(t) * B_x(t) - M_x(t) * B_z(t)) - \frac{M_y(t)}{T_2} \\
 \frac{dM_z(t)}{dt} &= \gamma(M_x(t) * B_y(t) - M_y(t) * B_x(t)) - \frac{M_z(t) - M_{eq}}{T_1}
 \end{aligned} \tag{2}$$

Here,  $\gamma$  is the Gyromagnetic ratio (Table 1),  $M_x, M_y$ , and  $M_z$  is the magnetization pointing in the x, y, and z directions, respectively, and  $B_x(t), B_y(t)$ , and  $B_z(t)$  describe the direction and size of the time-dependent magnetic field that the spin experiences.  $T_2$  describes transverse relaxation (signal loss), and  $T_1$  describes longitudinal relaxation (magnetization behaves differently for x and y as compared to z because we assume a large, static field points along the z-direction).  $M_0$  is the magnetization found along z at thermal equilibrium. We will simplify these equations to understand the individual terms below.

- The field  $(B_x(t), B_y(t), B_z(t))$  is taken to be time dependent, because we may apply an oscillating magnetic field to the sample (usually along x, so  $B_y(t) = 0$ ), using a coil, and have a large, fixed field along z ( $B_z(t) = B_0$ ). For simplicity, we eliminate the relaxation terms ( $T_2, T_1$ ) and start without an oscillating field ( $B_x(t) = B_y(t) = 0, B_z(t) = B_0$ ). Then, the Bloch equations simplify to:

$$\begin{aligned}
 \frac{dM_x(t)}{dt} &= \gamma B_0 M_y(t) \\
 \frac{dM_y(t)}{dt} &= -\gamma B_0 M_x(t) \\
 \frac{dM_z(t)}{dt} &= 0,
 \end{aligned} \tag{3}$$

where if we take the initial magnetization to lie along the x-axis ( $M_x(0) = M_0, M_y(0) = 0, M_z(0) = 0$ ), we obtain

$$\begin{aligned}
 M_x(t) &= M_0 \cos(\gamma B_0 t) \\
 M_y(t) &= -M_0 \sin(\gamma B_0 t) \\
 M_z(t) &= 0,
 \end{aligned} \tag{4}$$

as plotted in Figure 4A.

- If the applied field is static, the magnetization will always rotate around that field. In the above example, the field is along z, and so magnetization rotates about z, but the total field (represented by its components in the x,y, and z directions) may point in any direction, and this rule will still hold.
- One may also include  $T_1$  and  $T_2$  relaxation, by including the last terms in eq. 2, resulting in the following solution ( $M_x(0) = M_0, M_y(0) = 0, M_z(0) = 0$ ):

$$\begin{aligned}
 M_x(t) &= M_0 \cos(\gamma B_0 t) \exp(-t/T_2) \\
 M_y(t) &= -M_0 \sin(\gamma B_0 t) \exp(-t/T_2)
 \end{aligned} \tag{5}$$

$$M_z(t) = M_{eq}(1 - \exp(-t/T_1)) \tag{6}$$

$T_2$  is referred to transverse relaxation (perpendicular to the  $B_0$  field), and gradually destroys magnetization in the xy-plane (Figure 4B).  $T_1$  is referred to as longitudinal relaxation and describes recovery of magnetization to thermal equilibrium ( $M_0$ ). Nuclear spins have a slight preference for being either spin-up or spin-down (depending on the sign of  $\gamma$ , see Table 1). After some time, usually seconds, magnetization will recover to thermal equilibrium (Figure 4C/D). The equilibrium magnetization is what gives rise to signal in many NMR experiments (a variety of methods seek to generate greater magnetization than found at thermal equilibrium, as in dynamic nuclear polarization experiments, but these are usually less straightforward experiments).

## 2.2 Resonance

We may use the Bloch equations to understand the basics of magnetic resonance, and how we may control spin states using that resonance. In this section, we will omit relaxation ( $1/T_1 = 0, 1/T_2 = 0$ ), but apply a time dependent field in the x-direction, and see how this may be used to manipulate the state of the spin. In this case, the Bloch equations with only the relevant terms are

$$\begin{aligned}
 \frac{dM_x(t)}{dt} &= \gamma M_y(t) B_0 \\
 \frac{dM_y(t)}{dt} &= \gamma (2|B_1| \cos(\omega_{rf} t) M_z(t) - M_x(t) B_0) \\
 \frac{dM_z(t)}{dt} &= -2\gamma |B_1| \cos(\omega_{rf} t) M_y(t),
 \end{aligned} \tag{7}$$

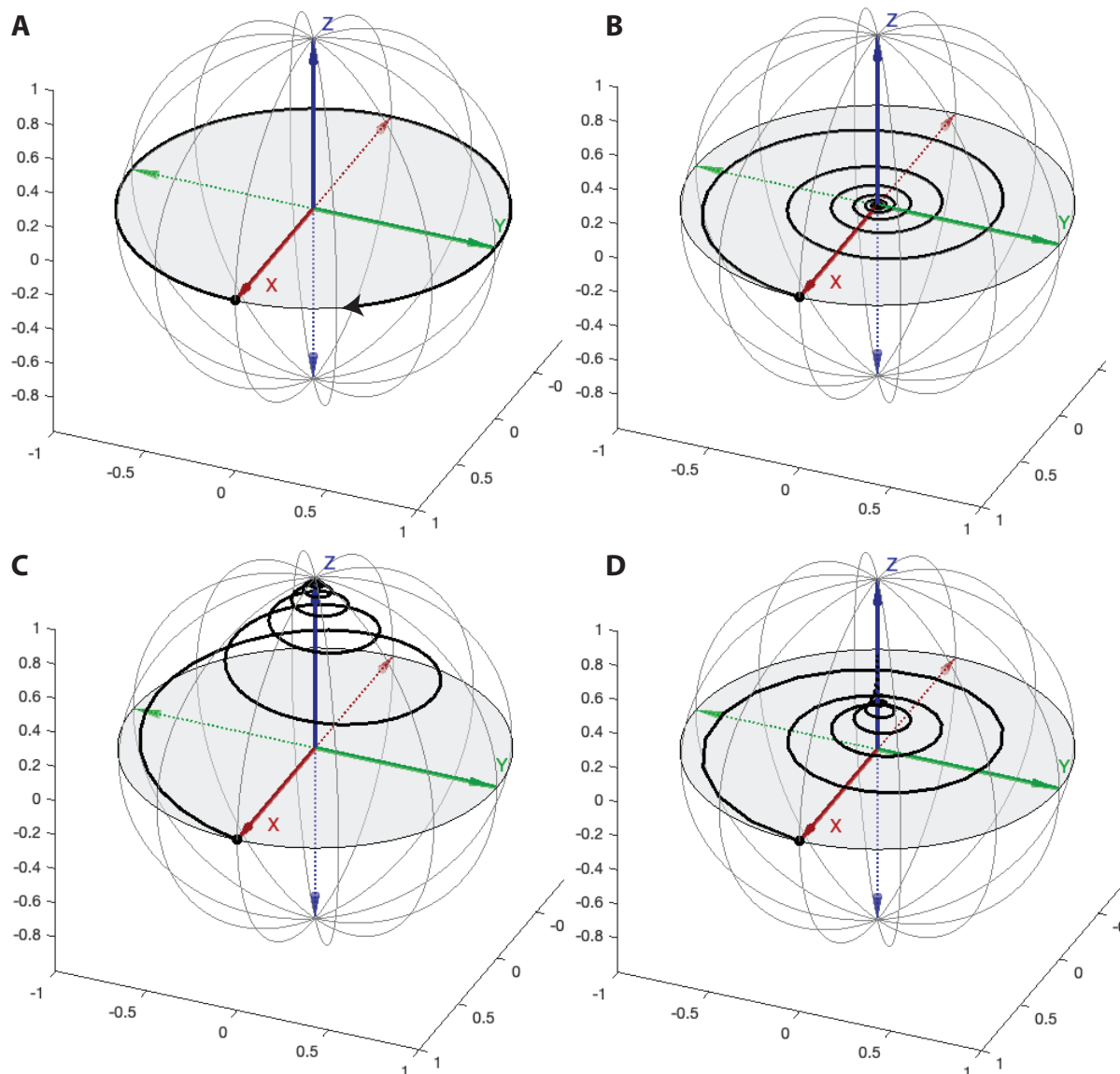


Figure 4: Trajectories of magnetization calculated using the Bloch equations. **A** Oscillation around a static  $B_0$  field. **B** Oscillation around  $B_0$  with  $T_2$  relaxation. **C** Oscillation around  $B_0$  with  $T_1$  and  $T_2$  relaxation ( $T_1 = T_2$ ). **D** Oscillation around  $B_0$  with  $T_1$  and  $T_2$  relaxation ( $T_1 = 10T_2$ ). **A-D** are provided as videos in wk1\_videos.ppt. Note that the relative sizes of the oscillation frequencies and  $T_1$ ,  $T_2$  are highly unrealistic for a real NMR experiment.

$2|B_1|$  is the amplitude of the oscillating field (the factor of 2 results in  $\gamma B_1$  yielding the effective oscillation frequency due to the  $B_1$  field).  $\omega_{rf}$  is the angular frequency of the oscillation. While this set of equations can be solved generally, we will discuss results for a few particular results.

- First, we consider what happens if the applied field ( $B_1$ ) does not oscillate, that is  $\omega_{rf} = 0$ . The  $B_0$  field causes rapid oscillation around z (Figure 4A). Noting that  $|B_1| \ll B_0$ , we find that the term  $2\gamma|B_1|M_y(t)$  rapidly cycles from positive to negative, so that  $dM_z(t)/dt$  is averaged to zero. Results are plotted for magnetization starting along the z-axis, with a static field applied in the z- and x-axes in 5A.
- On the other hand, we could apply the pulse on-resonance. This means, the oscillation frequency of the applied field matches the oscillation frequency re-

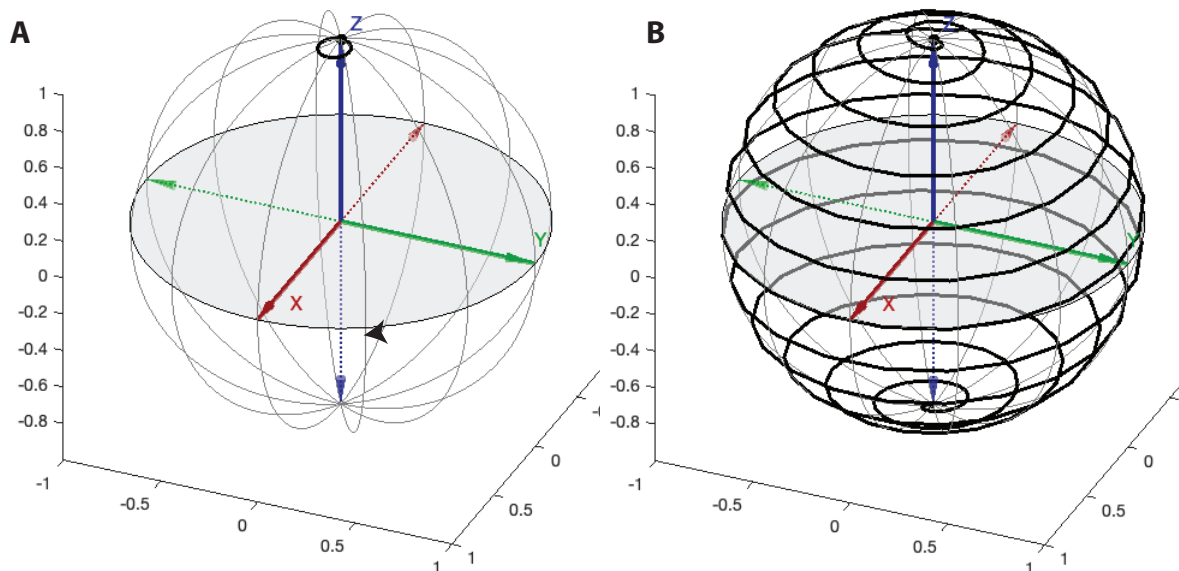


Figure 5: Trajectories of magnetization with an applied ( $B_1$ ) field. **A** plots a trajectory where  $B_1$  is static, resulting in only small deviations from the starting magnetization (for a more realistic  $B_1/B_0$  ratio (a smaller ratio), deviation would be invisible in this plot). **B** plots a trajectory where  $\omega_{rf} = \gamma B_0$ , that is, the pulse is on-resonance. This results in magnetization traveling from  $+z$  to  $-z$  (the  $180^\circ$  re-orientation is referred to as a  $\pi$ -pulse. A shorter application of the  $B_1$  field could be used to bring the magnetization to the  $xy$ -plane). See `wk1_videos.ppt`, slide 5 and 6 to see the trajectories as a video

sulting from the  $B_0$ , that is  $\omega_{rf} = |\gamma B_0|$ . In this case,  $M_x(t)$  and  $M_y(t)$  oscillate as given in eq. 4, but the applied field, given by  $2\gamma|B_1|\cos(\omega_{rf}t)$ , oscillates at the same frequency. The resulting evolution of the magnetization is:

$$\begin{aligned} M_x(t) &= M_0 \sin(\gamma B_0 t) \sin(\gamma |B_1| t) \\ M_y(t) &= M_0 \cos(\gamma B_0 t) \sin(\gamma |B_1| t) \\ M_z(t) &= M_0 \cos(\gamma |B_1| t), \end{aligned} \quad (8)$$

- This is the "resonance" in magnetic resonance- by applying an oscillating field at the same frequency that a spin oscillates in an external field, resonance is achieved. Although Rabi performed a very different experiment, with spin- $\frac{1}{2}$  particles traveling through field gradients, the oscillating field applied during the experiment achieved resonance in the same way (Figure 2).
- This allows us to manipulate spins selectively, for example,  $\gamma B_0$  depends on the nucleus (Table 1), so that using different irradiation frequencies allows one to manipulate different types of nuclei separately (ex.  $^1\text{H}$ ,  $^{13}\text{C}$ ,  $^{15}\text{N}$ ).
- Resonance is often understood using a so-called "rotating frame". The time-dependent  $B_1$  field is inconvenient when solving eq. 7. We develop a frame that rotates clockwise around the z-axis with the frequency of the applied  $B_1$  field, so that we can treat this field as a constant field along x. Consider how Figure 7B appears in this case: magnetization no longer rotates about z, but simply progresses from  $+z$  to  $-z$ , through the y-axis, as shown in Figure 6.

$$\begin{aligned}
 M_x(t) &= 0 \\
 M_y(t) &= M_0 \sin(\gamma|B_1|t) \\
 M_z(t) &= M_0 \cos(\gamma|B_1|t),
 \end{aligned} \tag{9}$$

as plotted in Figure 5B.

- Note that the applied field oscillates from  $2\gamma|B_1|$  to  $-2\gamma|B_1|$  along x, as opposed to actually rotating ( $x \rightarrow y \rightarrow -x \rightarrow -y \rightarrow$ ). In the rotating frame, this becomes

$$B_x(t) = \gamma|B_1|(1 + \cos(2\omega_{rf}t)) \approx \gamma|B_1|, \tag{10}$$

but the oscillating term has virtually no influence on the magnetization so it is discarded.

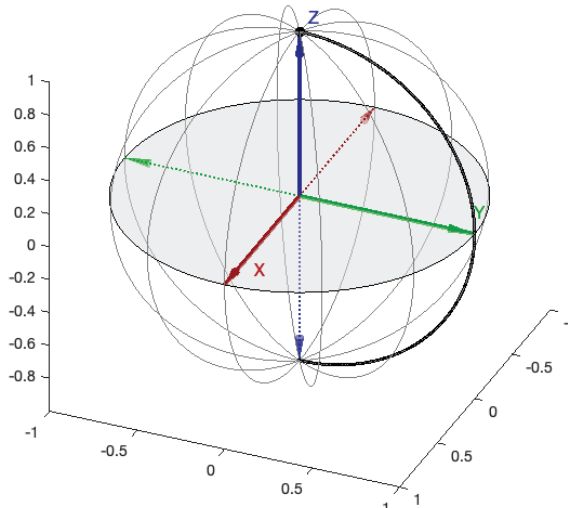


Figure 6: Trajectory of magnetization for an on-resonance pulse in the rotating frame (compare to Figure 5B). Also see wk1\_videos.ppt, slides 7-9, for a comparison of the trajectory in the lab and rotating frames.

- The Bloch equations may be written in the rotating frame, as follows (neglecting relaxation)

$$\begin{aligned}
 \frac{d\tilde{M}_x(t)}{dt} &= (\gamma B_0 - \omega_{rf})\tilde{M}_y(t) \\
 \frac{d\tilde{M}_y(t)}{dt} &= -(\gamma B_0 - \omega_{rf})\tilde{M}_x(t) + \gamma|B_1|\tilde{M}_z(t) \\
 \frac{d\tilde{M}_z(t)}{dt} &= -\gamma|B_1|\tilde{M}_y(t),
 \end{aligned} \tag{11}$$

- In the case of on-resonance irradiation,  $\gamma B_0 \pm \omega_{rf} = 0$ , so that oscillation around z vanishes entirely, and we only rotate around x, leading to the behavior in Figure 6.
- Note that we also now have a  $\gamma|B_1|$  as a static field, acting along x.
- We often refer to  $\pi/2$ -pulses and  $\pi$ -pulses which rotate magnetization either  $90^\circ$  or  $180^\circ$ , respectively. We also refer to "x" and "y" pulses, that is, the

"phase" of the pulse. We are referring to the direction in which the oscillating field is applied in the rotating frame (we always apply the pulse along the x-axis in the lab frame, see Figure 3B). In Figure 6, an x-pulse is applied, resulting in rotation around the rotating-frame's x-axis. A y-pulse would rotate magnetization around the rotating-frame y-axis. In the lab frame,  $B_y(t)$  remains 0 for both x- and y-pulses (we can't rotate the coil itself!), but has a different time dependence, that is  $B_x(t) = 2\gamma|B_1|\cos(\omega_{rf}t)$  for x-pulses and  $B_y(t) = 2\gamma|B_1|\sin(\omega_{rf}t)$  for y-pulses.

### 3 NMR interactions

In the previous section, we see that we can manipulate different types of spins (ex.  $^1\text{H}$ ,  $^{13}\text{C}$ ,  $^{15}\text{N}$ ) separately, by exploiting different resonance conditions of different spins. We also may apply different types of pulses (by changing the length, ex.  $\pi/2$  and  $\pi$ -pulses, or the phase, ex. x, y, -x, -y. This only touches the surface of the sophistication of NMR-spin manipulation, but further details are outside the scope of this course. Above, we look how a spin interacts with a magnetic field.

However, the net field seen by a spin is the result not only of the static  $B_0$  field or the oscillating  $B_1$  field, but also of several additional interactions. We discuss these interactions now, and how they can provide us information about the molecules containing them.

#### 3.1 Zeeman interaction

The Zeeman interaction is the interaction of a nucleus with the external magnetic field, and it depends only on the Gyromagnetic ratio and the applied field,  $B_0$ . The resonance frequency (that is, the energy divided by  $\hbar$ ) resulting from the Zeeman interaction is

$$\omega_Z = \gamma B_0, \quad (12)$$

and is typically 100s of MHz for  $^1\text{H}$  (this frequency is the result of the energy difference for a spin-up spin,  $m_I = 1/2$ , and a spin-down spin,  $m_I = -1/2$ ). The  $^{13}\text{C}$  Zeeman interaction is always  $\sim 1/4$  of  $^1\text{H}$ , and the  $^{15}\text{N}$  Zeeman interaction is  $\sim 1/10$  of the  $^1\text{H}$  Zeeman interaction. This makes it usually much larger than the other interactions discussed here. Note this oscillation frequency is often referred to as the Larmor frequency.

#### 3.2 Chemical Shift

Based on eq. 12, one might imagine that all spins of a given nucleus (ex. all  $^1\text{H}$ ) resonate at the same frequency. In fact, this was the expectation for some time [6]; W.C. Dickenson reported in 1950 that "most unexpectedly, it has been found for  $^{19}\text{F}$  the value of the applied magnetic field  $H_0$  for nuclear magnetic resonance at a fixed frequency depends on the chemical compound containing the fluorine nucleus" [7], and Proctor and Yu made the "surprising observation" that frequency of  $^{15}\text{N}$  nuclei "depended strongly on the chemical compound in which it was contained" [8].

- This unexpected variation of resonance frequencies of nuclei of the same type is the result of the chemical shift. Chemical shift causes the effective field experienced by a nuclear spin to be lower than the applied  $B_0$  field (therefore, we often refer to it as chemical "shielding").

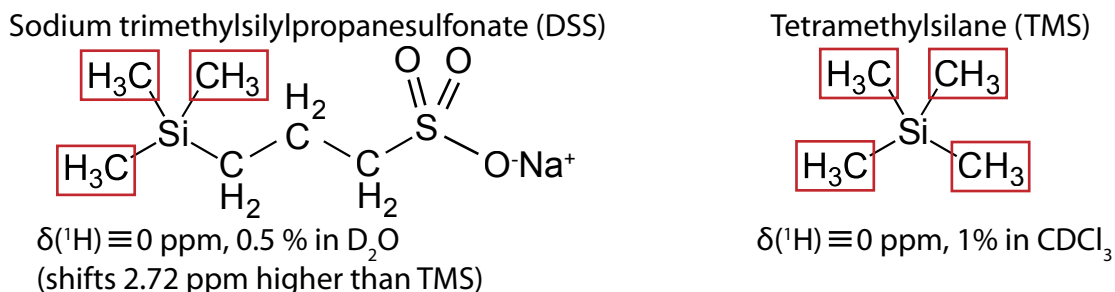


Figure 7: Molecules commonly used for chemical shift referencing. ppm scale is different, however, for these two molecules, where DSS referencing results in shifts 2.72 ppm lower than TMS.

- Chemical shift is a diamagnetic effect, that is, it is the dominant electron-nuclear interaction in systems where all electrons are paired in their orbitals. In such systems, no electron spin-alignment with a magnetic field is possible, since this would require the electrons to unpair (in contrast to paramagnetic and ferromagnetic systems). However, in a magnetic field, the electron spins do oscillate with the Larmor frequency of the electron. Then, they generate a small magnetic field pointing in the opposite direction to the external field (this is similar to electrons moving through a coil, which creates an electromagnet). The chemical shift generated is proportional to the Larmor frequency of the electrons, which is in turn proportional to the magnetic field ( $B_0$ ), so chemical shift is always proportional to  $B_0$ .
- Therefore, chemical shift is usually reported in parts per million (ppm), where typical values range from 0-200 ppm. This refers to the shift as a fraction of the Larmor frequency ( $\omega_L$ ), relative to a reference frequency. For example, if the  $^1\text{H}$  resonance frequency is 600 MHz (a 14.1 T magnet), and one reports a chemical shift of 5 ppm, this means that the observed frequency is  $5\text{ppm} \times (1 \times 10^{-6}/\text{ppm}) \times 600 \times 10^6 \text{Hz} = 3 \times 10^3 \text{Hz}$  higher than the reference compound's chemical shift. The change in frequency resulting from chemical shift is given by

$$\omega_{CS} = -\sigma\gamma B_0, \quad (13)$$

where  $\sigma$  is unitless, representing a fraction of the Larmor frequency (compare to eq. 12).

- Usually chemical shift is referenced to the methyl  $^1\text{H}$  shift of the TMS or DSS molecule ( $\delta \equiv 0$ ). Note, these two standards result in a different scale, since DSS shifts 2.72 ppm higher than TMS [9]. The TMS standard is usually used for measurement of organic molecules whereas DSS is more often used for proteins.
- Since chemical shift is brought about by shielding of nuclei by electronic orbitals, greater electron density results in a greater shielding. However, the parameter describing chemical shift (usually  $\delta$ ) is defined such that a greater shielding actually yields a lower ppm-value for  $\delta$ . Then, TMS and DSS, which are often defined to have  $\delta = 0$  ppm, have more electron density at the methyl  $^1\text{H}$ 's than most other compounds, so that negative  $^1\text{H}$  chemical shifts are rare using these referencing standards.
  - more  $e^-$  density  $\rightarrow$  more shielding  $\rightarrow$  lower frequency  $\rightarrow$  lower ppm-value
- Then, chemical shift tells us about the chemical environment near a nucleus. This results in many very useful trends for identifying NMR signals. We start

with organic compounds. For example,  $^1\text{H}$  shifts in ethanol can be seen in the NMR spectrum in Figure 8.

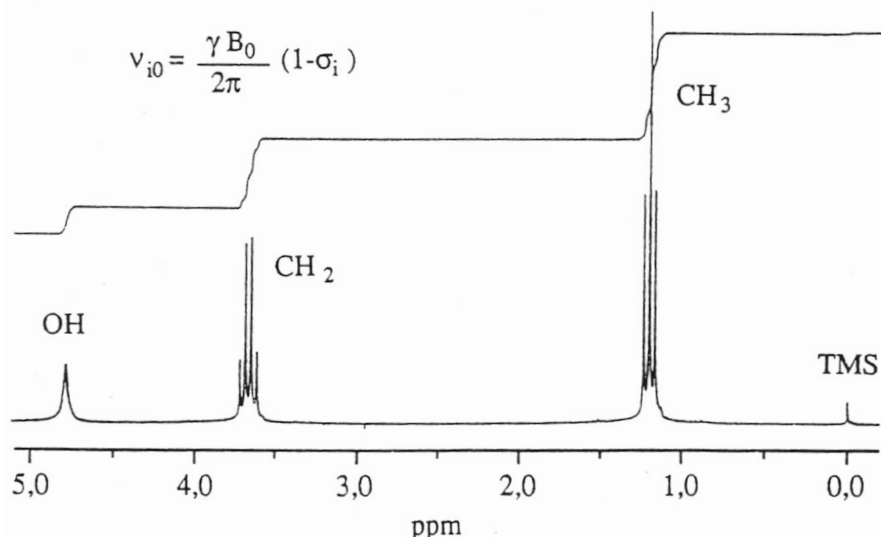


Figure 8: The O nucleus in ethanol is electron withdrawing, and so nearby  $^1\text{H}$  s are less shielded, resulting in higher chemical shifts. Referencing is to TMS. Splittings result from J-couplings, which are discussed in the next section.

- Trends in  $^1\text{H}$ ,  $^{13}\text{C}$ ,  $^{15}\text{N}$ , and  $^{31}\text{P}$  chemical shifts are plotted in Figure 9.
- $^1\text{H}$  and  $^{13}\text{C}$  shifts in proteins depend strongly on the position in the amino acid side chain ( $\alpha$ ,  $\beta$ ,  $\gamma$ , etc.) and to a lesser extend on the amino acid containing the protein, as shown in Figure 10.
- Dispersion of chemical shifts as a function of amino acid is insufficient to distinguish and assign resonances to particular amino acid types in proteins (although some amino acids, such as Glycine or Threonine can usually be identified). However, if one can determine that a set of  $\text{C}\alpha$  shifts are sequential in a protein (sometimes with  $\text{C}\beta$ ), it is usually possible to determine where that set of shifts belongs in the protein sequence. This will be discussed further next week.
- Chemical shift also provides some structural information. For example, the  $^{13}\text{C}\alpha$  chemical shift in amino acids tends to shift to higher ppm values when the amino acid is in an  $\alpha$  helix, and lower values when in a  $\beta$  sheet. Conversely,  $\delta(^{13}\text{C})$  of  $\text{C}\beta$  shifts towards lower ppm values in  $\alpha$ -helices and higher values in  $\beta$ -sheets. This is plotted in Figure 11A. For this reason, one often calculates the "secondary"  $^{13}\text{C}$  chemical shift, defined as the measured chemical shift minus the average chemical shift for that amino acid type and carbon ( $\Delta\delta(^{13}\text{C})$ ). Since the secondary chemical shift goes in opposite directions for  $\text{C}\alpha$  and  $\text{C}\beta$ , this is taken a step further and one calculates the difference of the secondary  $\text{C}\alpha$  and  $\text{C}\beta$  chemical shifts (11B).

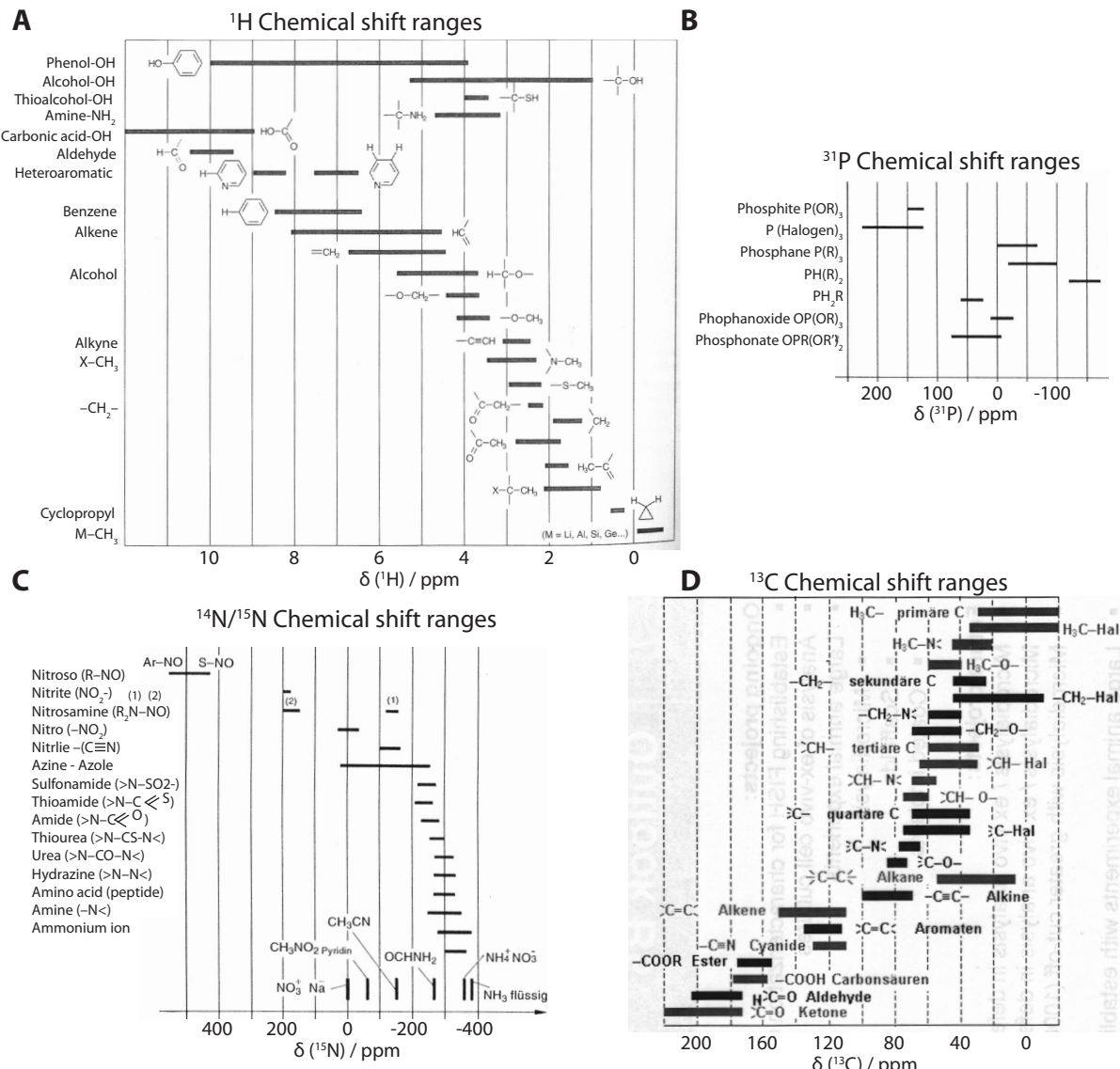


Figure 9: Chemical shift ranges for different chemical groups for common nuclei ( $^1\text{H}$ ,  $^{13}\text{C}$ ,  $^{15}\text{N}$ ,  $^{31}\text{P}$ ). A more common referencing scheme defines liquid Ammonia as having  $\delta(^{15}\text{N}) \equiv 0$  ppm.

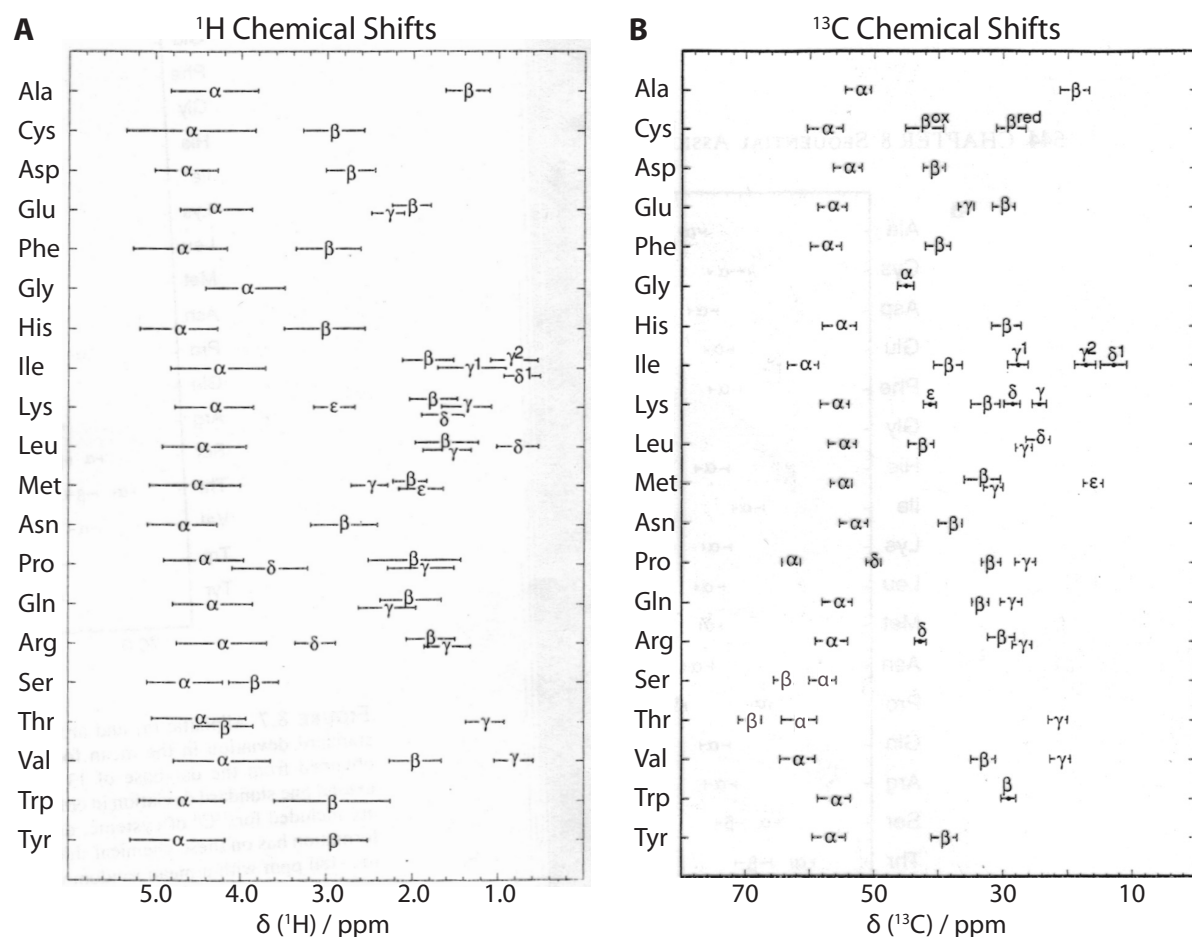


Figure 10: Chemical shift ranges for different amino acids at the various positions in the side chain. Bars indicate one standard deviation of the chemical shift.

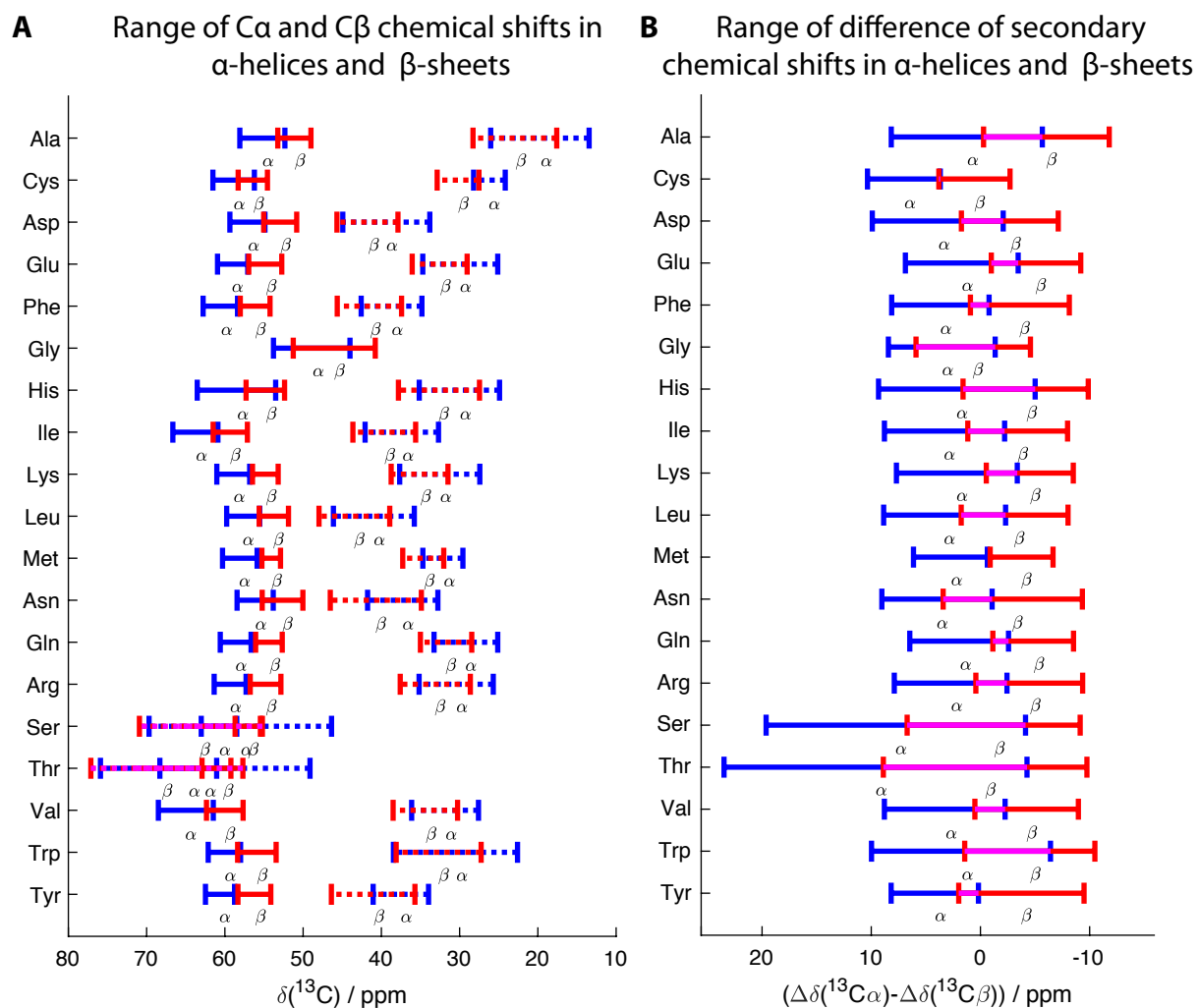


Figure 11: Secondary chemical shift. **A** Chemical shift ranges for different amino acids in  $\alpha$ -helices (blue) and  $\beta$ -sheets (red) for  $\delta^{13}\text{C}\alpha$  and  $\delta^{13}\text{C}\beta$ . **B** Range of  $\Delta\delta^{13}\text{C}\alpha - \Delta\delta^{13}\text{C}\beta$  for  $\alpha$ -helices and  $\beta$ -sheets.

### 3.3 Dipolar coupling

Dipolar couplings are the result of a through-space interaction between two spins. Therefore, the dipole interaction can be understood fairly well as the quantum equivalent of the interaction of two bar magnets (Figure 12). That is, the energy of the interaction depends on the distance of the two spins, the angle of the two spins, and whether the spins are spin-up and spin-down ( $m_I = \pm 1/2$ ). The change in resonance frequency of a given spin depends on the state of the second spin ( $m_I \pm 1/2$ ), resulting in a splitting of width

$$\omega_D = \frac{\mu_0}{4\pi} \frac{\gamma_1 \gamma_2 \hbar}{r_{12}^3} \frac{3 \cos^2(\theta) - 1}{2}, \quad (14)$$

where  $\mu_0$  is a constant (the permeability of free space),  $r$  is the distance between the two spins, and  $\theta$  is the angle between the two spins (relative to the direction of the magnetic field,  $B_0$ ). Note, this equation is only valid for a pair of heteronuclear spins (ex.  $^1\text{H}$  and  $^{13}\text{C}$ , but not  $^1\text{H}$  and another  $^1\text{H}$ ). Calculating splitting between homonuclear spins requires a full quantum mechanical treatment.

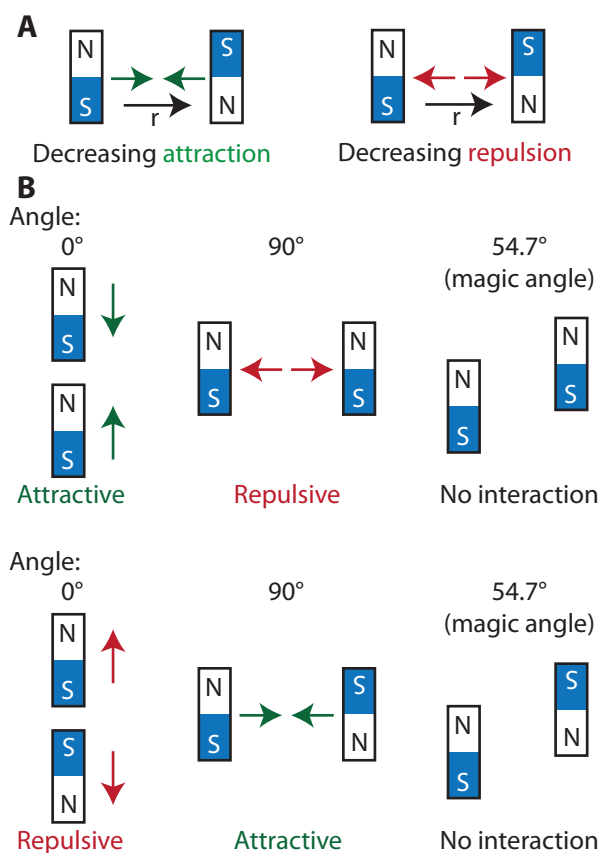


Figure 12: Interactions of two bar magnets. **A** If the two magnets become more distant in space, the magnetic force between them is reduced, although the direction of the force depends if the two magnets point in the same direction or in opposite directions. **B** The interaction also depends on the angle connecting them. If the magnets point in the same direction, and are aligned vertically, they experience an attractive force, but if they are aligned horizontally, force becomes repulsive. In between 0° and 90°, the force vanishes (at 54.74°). Switching the direction of one of the magnets reverses the direction of the force.

Note that in solution-state NMR, we do not observe the dipole coupling directly. A molecule "tumbles" in solution, which means that it randomly samples all possi-

ble orientations, so that that the orientational dependence of the dipole coupling causes this interaction to vanish. However, it will later play a role in NOE transfers for structure determination (week 3).

### 3.4 J-coupling

In contrast to dipole couplings, J-couplings are the result of through-bond interactions between nuclear spins. We often refer to these as "scalar" couplings, because while molecular tumbling eliminates the dipole coupling, the J-coupling is non-zero when motionally averaged. Usually, only this average value can be determined experimentally.

- J-couplings between protons are mediated by electrons, via the electron-nuclear coupling (Hyperfine coupling). The state of a nuclear spin ( $m_I \pm 1/2$ ) affects the oscillation frequency of the electrons near it via the hyperfine coupling. This increases or decreases the field induced by that electron, and therefore changes the total field experienced by other spins near that electron (similar to  $B_0$  causing an induced field from the electrons, resulting in chemical shift).
- Similar to the chemical shift, J-couplings contain structural information. For example, the Karplus equation parameterizes the J-coupling based on dihedral angles ( $\theta$ ):

$$J = A \cos^2(\theta) + B \cos(\theta) + C, \quad (15)$$

where  $A$ ,  $B$ , and  $C$  are determined from experiment (ex.: Figure 13). Then, one can use the Karplus equation and measured J-couplings to determine dihedral angles in a molecule.

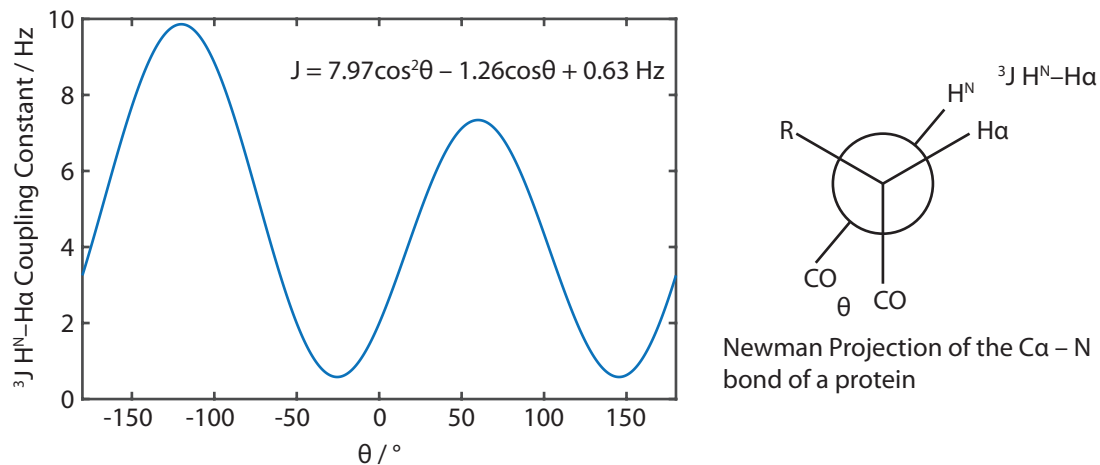


Figure 13: The Karplus equation for  $^3J_{\text{HN}-\text{H}\alpha}$  couplings.

- J-couplings manifest in a spectra as peaks that have been split into two or more additional peaks. Then, the resonance of an NMR active spin near to another nucleus with non-zero spin will yield multiple lines (although heteronuclear decoupling methods may be used to remove this effect, for example, a  $^{13}\text{C}$  spectrum may use  $^1\text{H}$  decoupling, so splittings from nearby  $^1\text{H}$  are not observed).

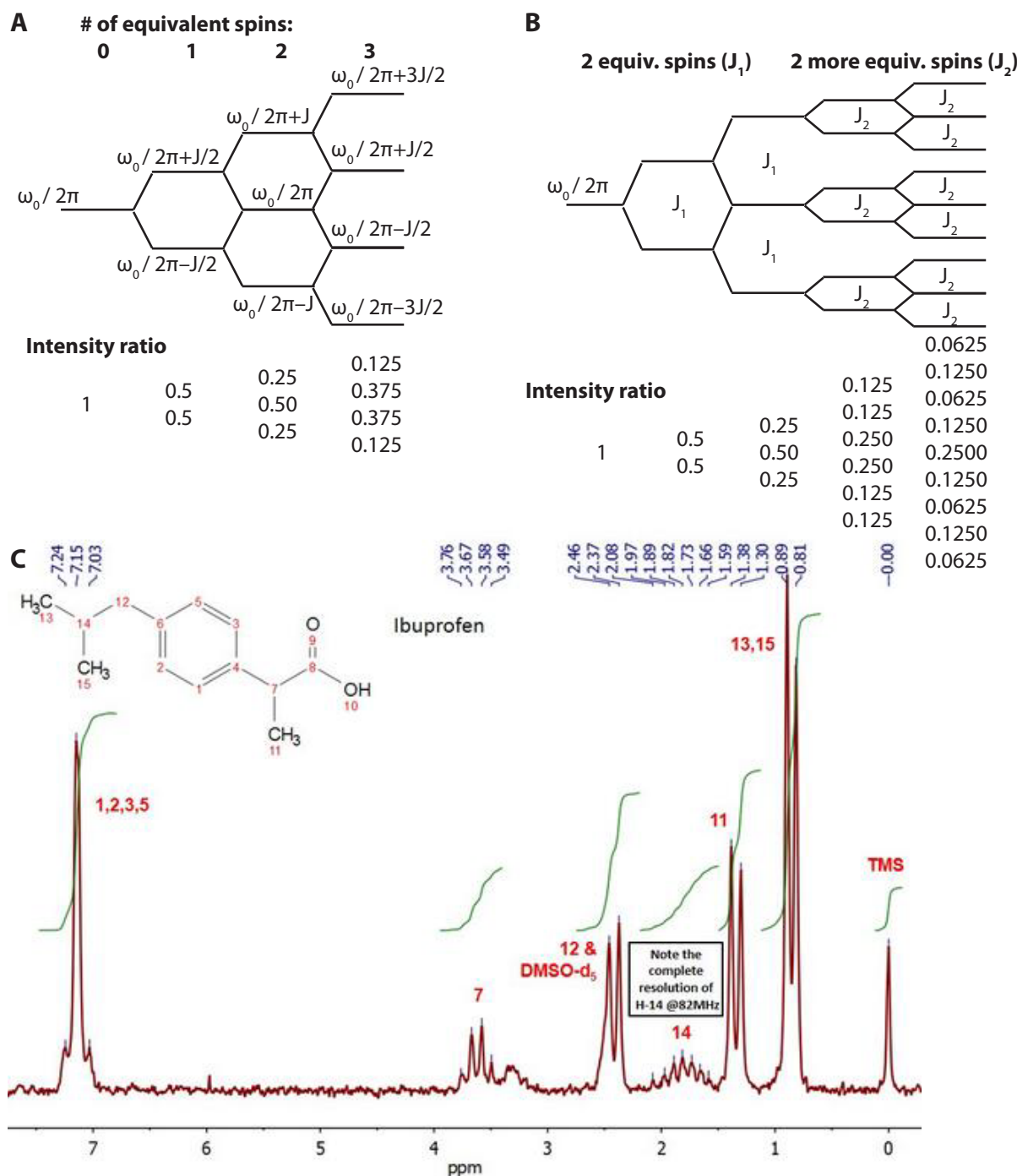


Figure 14: Multiplicity in J-splittings. **A** shows the multiplets resulting from splitting of a spin by three equivalent spins. **B** shows multiplets resulting from splitting of a spin first by two equivalent spins, and then a second pair of equivalent spins (different than the first pair). **C** shows an assigned spectrum of ibuprofen, where various multiplets are observed due to the J-couplings between  $^1\text{H}$  on neighboring atoms.

- The multiplicity of a peak in  $^1\text{H}$  spectra, that is, the number of times it has been split by J-couplings can be used to help in assignment of small molecules, by providing information about neighboring atoms. Take the ethanol spectrum in Figure 8. The resonance corresponding to the  $\text{CH}_3$  group is split into 3 peaks, because these 3  $^1\text{H}$  neighbor 2 equivalent  $^1\text{H}$  on the  $\text{CH}_2$  group (the rule is  $n + 1$  peaks when neighboring  $n$  equivalent nuclei, equivalent  $^1\text{H}$  are usually meaning bonded to the same carbon, although may also be equivalent by

symmetry). This is illustrated in Figure 14.

- Note that J-couplings between two equivalent spins (ex. on the same carbon) are in typical cases not visible in NMR spectra.

### 3.5 Other interactions

We've neglected a number of interactions which should be briefly mention (although these will not come up in this course)

1. **Quadrupole coupling** Coupling that influences the energy levels of spin systems with  $I > 1/2$  (these nuclei couple to themselves. One can also think of this as the multiple spin-1/2 protons and neutrons couple to each other and bring about the quadrupole coupling).
2. **Hyperfine coupling** Splitting resulting from the coupling between a nuclei and an unpaired electron.
3. **Pseudocontact shift** Coupling between a nuclei and an electron that results in a small shift of the nuclear frequency (not a splitting), and is the results of rapid averaging of the hyperfine coupling due to electron flips from  $m_S = -1/2$  to  $m_S = +1/2$ .

### Next week

While one can often assign or identify small molecules using one-dimensional  $^1\text{H}$  and/or  $^{13}\text{C}$  NMR, we are interested in characterizing proteins using NMR. 1D spectra for proteins are much too complicated to separate all resonances and learn much about the protein, as one can see in a  $^1\text{H}$  spectrum of ubiquitin in Figure 15. Therefore, we will need to use higher dimensional spectra, first to assign various  $^1\text{H}$  ,  $^{13}\text{C}$  , and  $^{15}\text{N}$  resonances, and later to obtain structural information.

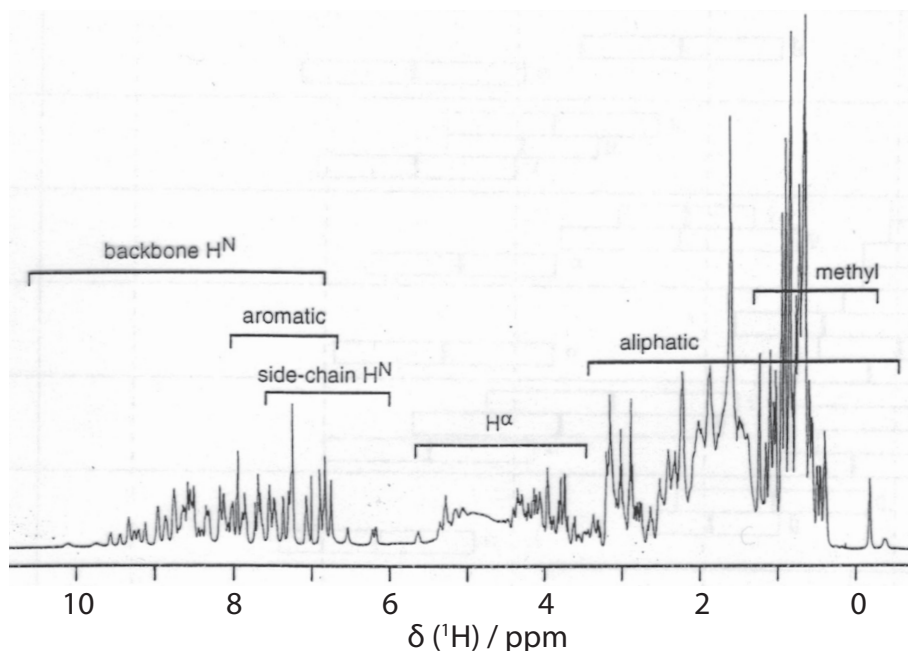


Figure 15: Ubiquitin 1D  $^1\text{H}$  spectrum.

## References

- [1] W. Gerlach and O. Stern, "Der experimentelle nachweis der richtungsquantelung im magnetfeld.", *Zeitschrift für Physik*, vol. 9, no. 1, pp. 349–352, 1922.
- [2] W. Pauli, "Über den zusammenhang des abschlusses der elektronengruppen im atom mit der komplexstruktur der spektren," *Zeitschrift für Physik*, vol. 31, pp. 765–783, 1925.
- [3] N. Straumann, "The Role of the Exclusion Principle for Atoms to Stars: A Historical Account," *arXiv e-prints*, pp. quant-ph/0403199, Mar. 2004.
- [4] I. I. Rabi, J. R. Zacharias, S. Millman, and P. Kusch, "A new method of measuring nuclear magnetic moment," *Phys. Rev.*, vol. 53, pp. 318–318, Feb 1938.
- [5] F. Bloch, "Nuclear induction," *Phys. Rev.*, vol. 70, pp. 460–474, Oct 1946.
- [6] S. G. Levine, "A short history of the chemical shift," *J. Chem. Ed.*, vol. 78, no. 1, p. 133, 2001.
- [7] W. Dickenson *Phys. Rev.*, vol. 77, pp. 736–737, 1950.
- [8] W. Proctor and F. Yu *Phys. Rev.*, vol. 77, p. 717, 1950.
- [9] R. K. Harris, E. D. Becker, S. M. C. De Menezes, P. Granger, R. E. Hoffman, and K. W. Zilm, "Further conventions for nmr shielding and chemical shifts (iupac recommendations 2008)," *Magnetic Resonance in Chemistry*, vol. 46, no. 6, pp. 582–598, 2008.